The use of centrifuge modelling to investigate progressive failure of overconsolidated clay embankments

W.A. Take & M.D. Bolton
Cambridge University Engineering Department

ABSTRACT: Three technologies have been applied to the centrifuge modelling of clay embankments including matric suction measurement, an environmental chamber, and image-based deformation measurement. Using these technologies, a "rubblisation" failure mode has been observed in response to rainfall infiltration. The failure mode is described within the framework of presenting the challenges involved in modelling the observed behaviour numerically.

1 INTRODUCTION

Delayed failure of embankments and cut slopes has the potential to pose risk to human life, and cause great disruption to transportation infrastructure. Many of the reported failures occur after periods of wet weather, indicating an interaction between the environment, the resulting transient pore pressures, and slope stability.

Research into the failure of clay embankments and cut-slopes has largely taken the form of limit equilibrium and finite element (e.g. Potts et al. 1990) back-analyses of slope failures, and numerical analysis assuming the significance of certain parameters governing rate effects (e.g. Alonso et al. 1995, Potts et al. 1997). The difficulty associated with measuring soil suctions, and the limitations associated with conventional "target-based" methods of deformation measurement have restricted the full application of physical modelling techniques to observe rainfall-induced instability under controlled laboratory conditions.

2 EXPERIMENTAL METHODOLOGY

Three technologies have been developed to model the stability of overconsolidated clay embankments more accurately during rainfall infiltration in the centrifuge. These technologies improve the ability to measure matric suctions, to control the environmental boundary conditions surrounding the slope, and to observe soil deformation without the recourse to embedded target markers.

2.1 *Matric suction probe*

Effective stress analysis of any observed embankment behaviour requires the knowledge of the pore water pressures within the model embankment. Recent advances in the technology of direct measurements of negative pore water pressures have indicated that the key design features of such a device are the elimination of spaces likely to trap cavitation nuclei, a small water reservoir, a high air-entry porous element, and an effective saturation procedure (Ridley 1993, Guan and Fredlund 1997). A miniature matric suction probe based on these design criteria has been developed for use in centrifuge models. With a nominal 3 bar air-entry ceramic filter, and a rig-

orous programme of ceramic saturation, the probe is capable of measuring negative pore water pressure to a value of -400kPa.

2.2 *Environmental chamber*

Results from centrifuge testing, like all modelling exercises, are susceptible to errors due to incorrect boundary conditions. For the modelling of clay embankments, one often-overlooked boundary condition is that of the relative humidity above the embankment surface. If the air above the model embankment is allowed to be exchanged with dry air from the centrifuge chamber, the embankment will tend to lose moisture over time. Such a moisture loss will lead to the development of matric suctions and associated increases of effective stress within the clay. Settlements due to self-weight consolidation will be enhanced by those associated with shrinkage. The conventional environmental boundary condition, therefore, has the consequence that the pore pressures within the centrifuge model will not come into a state of equilibrium within the practical time frame of centrifuge modelling.

An environmental chamber has been designed to impose appropriate environmental boundary conditions on centrifuge models of clay embankments (Figure 1a). The chamber is sealed to prevent moisture transfer from the model to the external surroundings, and has the capability to regulate the relative humidity of the air in the chamber, and subject the embankment to model rainfall from atomising mist nozzles.

2.3 *Image-based deformation measurement*

An image-based system of deformation measurement system has been developed, both for use at 1-g and in the centrifuge, based on the techniques of Particle Image Velocimetry (PIV) (White et al. 2001a). This technique relies on the texture (i.e. a map of pixel intensities) of a patch of soil to identify the patch in a second image corresponding to a following time step (Figure 1b). Once the position of best-match is identified to sub-pixel accuracy, the difference between the location of the patch in two successive images is the displacement vector of the patch. Using this technique, deformations can be measured to a precision finer than $1/10^{th}$ of a pixel both in soils which have an inherent texture due to a large (i.e. visible) grain size and in fine-grained soils onto which a texture has to be applied (White et al. 2001b).

The use of image-based deformation measurement has the benefit that the measurement points need not be decided before the event occurs. In this manner, patches can be arranged to straddle a shear surface, for example, to monitor the strain mobilised along the length of the discontinuity during progressive failure. The effort involved with embedding target markers into clay models at equally spaced intervals has historically restricted the number of measurement points. Image-based deformation measurement, therefore, has the additional benefit of allowing thousands of displacement measurement points, thereby allowing the capture of shear strain localisation.

To minimise the effective pixel size over the area of interest at an economical price, a multi camera image acquisition system has been developed to capture digital images of various areas of interest in the centrifuge model at a resolution of 1760x1168 pixels. The multi-camera system is shown in Figure 1a, with the resulting camera views displayed in Figure 1b. The multiple digital cameras are controlled using a scalable scheduling engine written in Visual Basic based on the Kodak ActiveX software development kit for the DC240/280/3400/5000 family of consumer-level digital still cameras. Once captured, the images are quickly transferred to a computer in the low-g environment at the centre of the beam centrifuge before the cycle is repeated.

Image calibration provides the translation rule to convert deformations from image-space (pixels) to real space (mm) using the principles of close-range photogrammetry. The eighteen variables used in the calibration process include, but are not limited to, corrections for lens distortion, camera orientation, and refraction through the observation window. Despite the observed relative rotation with respect to the camera CCD of the camera lens under its own elevated self-weight, the process of camera calibration can correct the movement of soil patches by accounting for the apparent movement and distortion of stationary control points (White et al.

2001a). Finally, a mapping rule is applied to convert the curved embankment geometry as tested in a radial acceleration field to its equivalent in a parallel acceleration field.

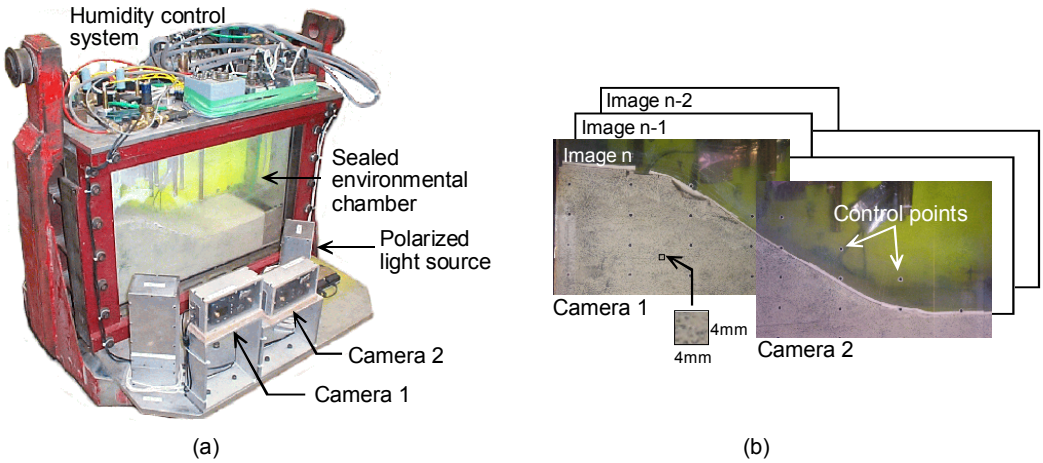

Figure 1. (a) Environmental chamber and multi-camera image acquisition system, and (b) the resulting view of the slope

3 RESULTS

The E-grade Kaolin clay used to create the model embankment was consolidated to a pressure of 500 kPa from slurry mixed at 100% moisture content. The resulting block of clay was shaped to form an embankment, underwent suction probe installation, and was inserted into the environmental chamber at a suction of 40 kPa. The clay embankment was then subjected to destabilising influences due to cycles both of increased acceleration level and of rainfall infiltration. The resulting change in embankment geometry resulting from a combination of these actions is presented in Figure 2. The original 36° slope was reduced to an angle of 30°, with a drop in the embankment surface elevation of 6.9 mm, corresponding to a field scaled displacement of 414 mm at 60g.

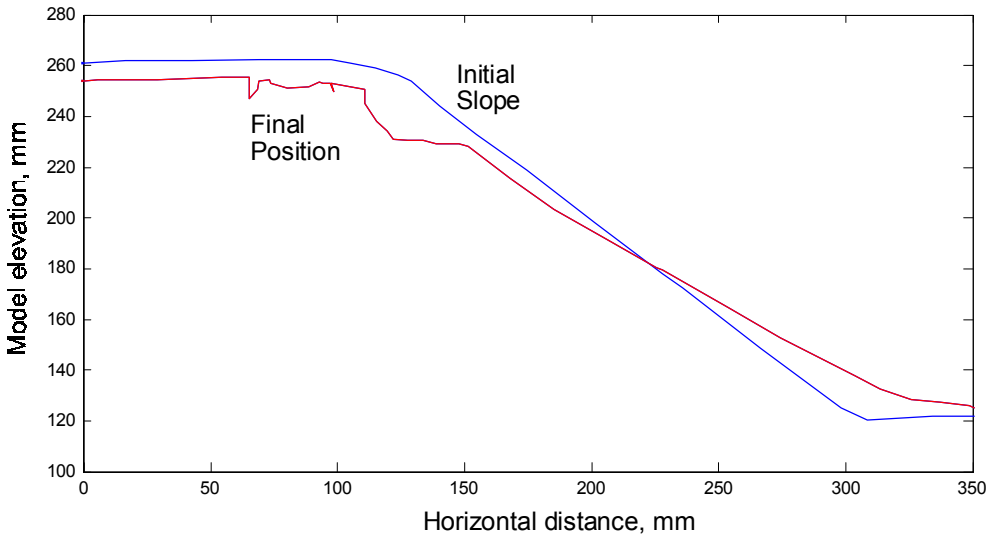

Figure 2. Embankment deformation observed in centrifuge model

3.1 *Failure due to acceleration level*

Much of the early work on centrifuge modelling of slope failures was performed by increasing the acceleration level until an undrained failure was observed. The gravity 'turn-on' technique of such a centrifuge test produced dramatic results and did not require complicated excavation or surcharging systems to bring the slope to failure. Based on the observed failure, the undrained strength of the clay could be then be back-calculated.

The 140 mm high model embankment in the current study was rapidly accelerated to 60g, causing the generation of excess pore pressures, thereby leading to some slope instability. Upon reaching an acceleration level of 60g, a failure mechanism was initiated by a crack forming at the crest of the embankment, which propagated with depth until a slip surface formed from the apex of the crack. The shear surface is very pronounced at the crest of the embankment, but gradually disappears with depth. The embankment deformations associated with this failure mechanism, as measured over 52 minutes of centrifuge testing, are shown in Figure 3. Following this slope instability, the embankment once again regained slope equilibrium and stopped deforming. This is consistent with the nature of the method in which the pore pressures were heightened. The excess pore pressures are at their maximum value at the moment the centrifuge acceleration is increased. For a relatively permeable clay embankment constituted from E-grade Kaolin, the fast dissipation of the pore water pressures leads to the embankment quickly stabilising.

The heightened pore pressures provoked by increasing the acceleration level do not model the potential increase in pore water pressures due to rainfall infiltration. As shown in Figure 3, the failure due to increasing the acceleration level will tend to be deep, and may not be driven to complete collapse. Although centrifuge models of slope instability brought about by increasing the acceleration level may behave according to the correct scaling laws, they do not necessarily reflect reality.

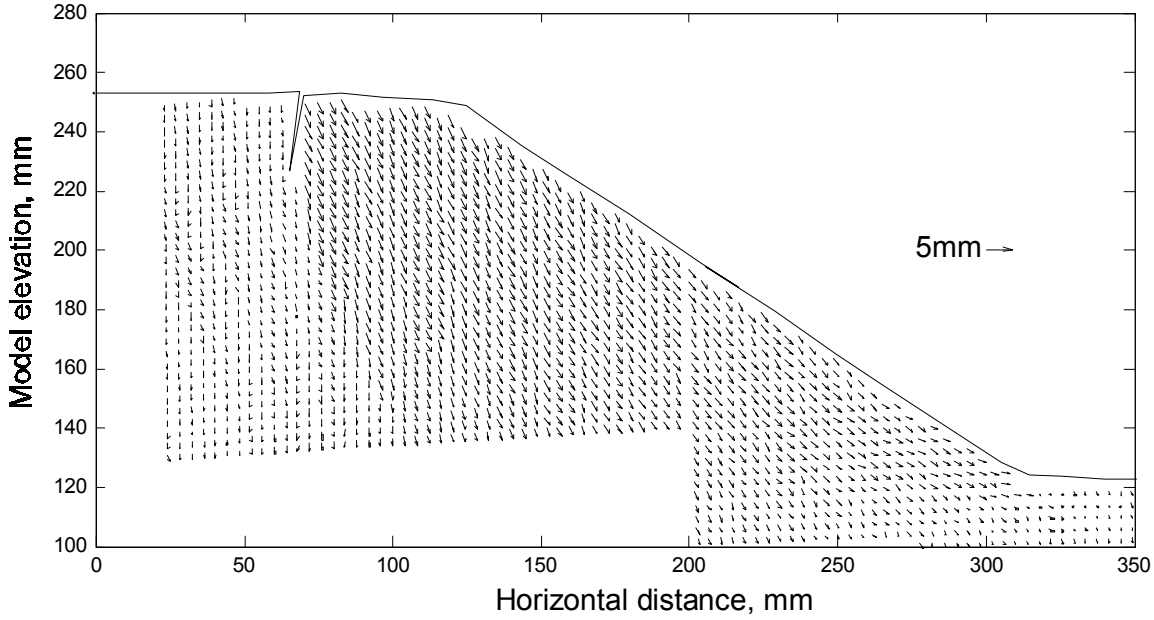

Figure 3. Observed embankment deformations associated with gravity 'turn-on' technique

3.2 *Failure due to rainfall infiltration*

Following the initial instability due to elevated g-level, the embankment was allowed to consolidate, with no additional deformations being observed on the initial failure surface. With the water table being held below the base of the embankment, and negligible moisture loss to the external environment, the pore pressures approached values of negative hydrostatic conditions. These suctions were then eliminated by the application of rainfall infiltration over the entire slope. Despite elevating the pore pressures to positive values everywhere in the embankment,

only small deformations were observed. After a period of extended, continuous model rainfall, a second tension crack was formed at the crest. The deformations measured during a period of 11 minutes just prior to, and following the tension crack formation are shown in Figure 4. The deformations presented in Figure 4, therefore, do not present a complete deformation history of the embankment, but rather, a snapshot of the onset of the second instability event. The second tension crack propagated until such depth that a slip surface developed with a corresponding increase in down-slope displacements.

Shortly after the mechanism of Figure 4 formed, a third tension crack appeared at the crest, movement along the existing failure surface ceased, and the down-slope velocity was transferred to a new failure surface (Figure 5). The resulting failure surface observed over 10 minutes was also non-circular and extended slightly deeper at the toe.

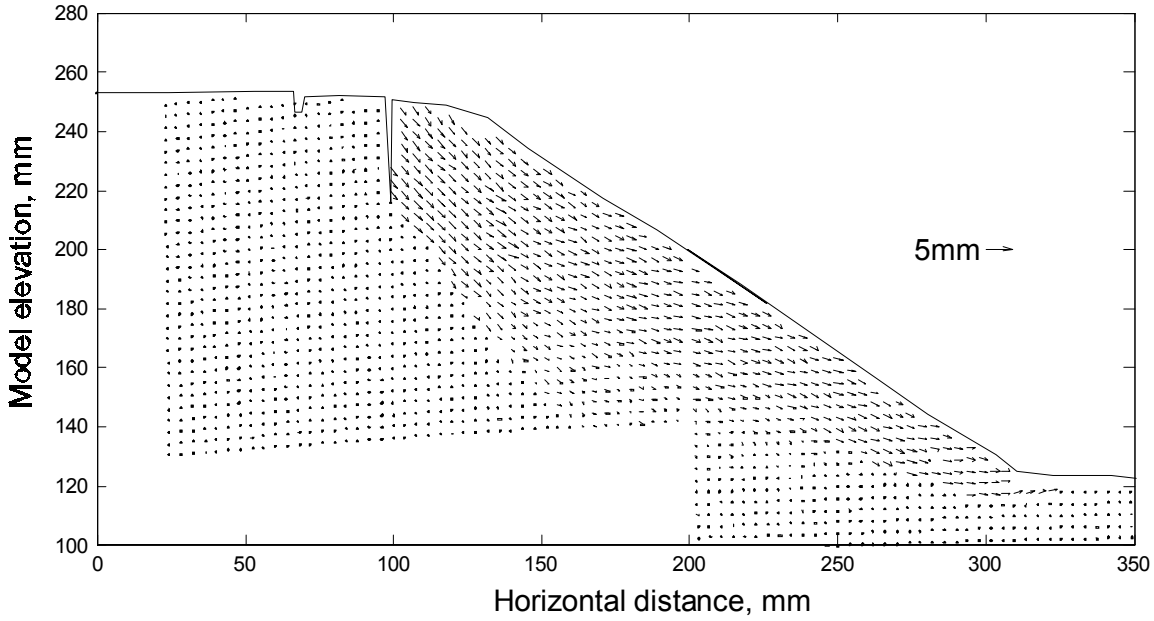

Figure 4. Rainfall induced embankment deformations

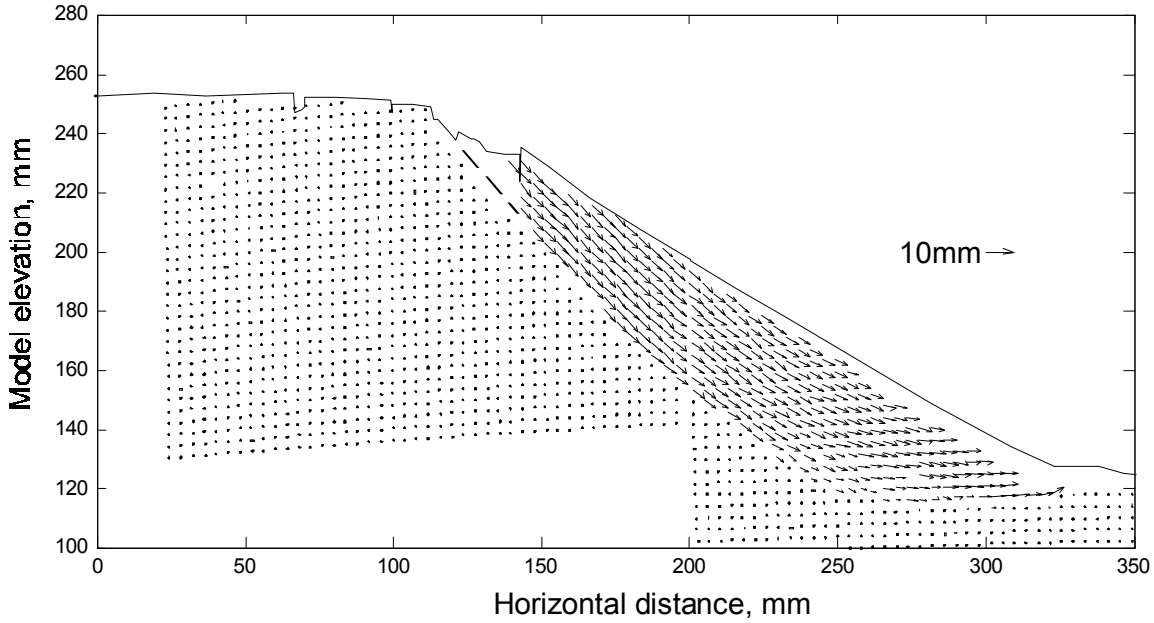

Figure 5. Deformations associated with continuing rubblisation of embankment slope

4 DISCUSSION

The series of cracks and failure surfaces observed in the clay embankment together form a 'rubblisation' failure mode in which the embankment material slowly breaks up and softens. Despite the series of these rubblisation failures, the slope still retained an angle of 30° at the completion of testing. It would be unrealistic to assume, therefore, that the rubblisation process had been carried out to its final state.

The observed rubblisation failure mode has important consequences for the design of retrofit measures for embankment stabilisation. For example, if the design of a retrofit scheme is based on soil strengths obtained from a back-analysis of a previous shallow slope failure, the rubblisation failure mode indicates that the strengths may fall to a lower value in the future. Although the calculated strengths are representative of the strength mobilised during a shallow slope failure, they may be higher than the fully softened strength of the material.

Each of the three failures presented in this paper displayed tension cracking at the crest of the embankment. The accurate modelling of the tensile strength of the clay as well as the rainfall infilling of the tension cracks would be difficult within a numerical modelling framework. In addition, the interaction and the relevant strength parameters on each of the dormant and active slip surfaces are arguably beyond the state-of-the-art of numerical modelling. Despite these difficulties, there exists a need to design embankment retrofits. This presents a significant challenge for numerical modelling.

5 CONCLUSIONS

High quality displacement measurement technology, the ability to measure soil suctions, and strictly controlled boundary conditions allow the investigation of progressive failure in overconsolidated embankments using centrifuge tests. A rubblisation failure mode has been observed to form during rainfall infiltration in which a series of tension cracks and shear surfaces form as the embankment material softens. The complexity associated with this failure mode would present a considerable challenge to current numerical modelling codes.

REFERENCES

Alonso, E., Gens, A. & Lloret, A. 1995. Effect of rain infiltration on the stability of slopes. In *Unsaturated Soils: Proceedings of the 1st International Conference on Unsaturated Soils, Paris*: 241-249. Rotterdam: Balkema.

Guan, Y. & Fredlund, D.G. 1997. Use of the tensile strength of water for the direct measurement of high soil suction. *Canadian Geotechnical Journal* 34: 604-614.

Potts, D.M., Dounais, G.T. & Vaughan, P.R. 1990. Finite element analysis of progressive failure of Carsington Embankment. *Geotechnique* 40(1): 79-101.

Potts, D.M., Kovacevic, N. & Vaughan, P.R. 1997. Delayed collapse of cut slopes in stiff clay. *Geotechnique* 47(5): 953-982.

Ridley, A.M. 1993. The measurement of soil moisture suction. Ph.D. dissertation, Imperial College, London.

White D. J., Take W.A., Bolton M.D. & Munachen S.E. 2001a. A deformation measuring system for geotechnical testing based on digital imaging, close-range photogrammetry, and PIV image analysis. *Proc. 15th Int. Conf. Soil Mechanics and Geotechnical Engineering*, *Istanbul, Turkey.*

White D.J., Take W.A. & Bolton M.D. 2001b. Measuring soil deformation in geotechnical models using digital images and PIV analysis. In Chandra Desai et al. (eds.), *Proc. 10th Int. Conf. Computer Methods and Advances in Geomechanics. Tucson, Arizona*: 997-1002. Rotterdam: Balkema.